Cystatin M/E is a high affinity inhibitor of cathepsin V and cathepsin L by a reactive site that is distinct from the legumain-binding site

Cheng, Tsing; Hitomi, Kiyotaka; Van Vlijmen-Willems, Ivonne M.J.J.; De Jongh, Gys J.; Yamamoto, Kanae; Nishi, Koji

Published in:
Journal of Biological Chemistry

DOI:
10.1074/jbc.M600694200

Publication date:
2006

THE JOURNAL OF BIOLOGICAL CHEMISTRY VOL. 281, NO. 23, pp. 15893–15899, June 9, 2006

Cystatin M/E Is a High Affinity Inhibitor of Cathepsin V and Cathepsin L by a Reactive Site That Is Distinct from the Legumain-binding Site

*A NOVEL CLUE FOR THE ROLE OF CYSTATIN M/E IN EPIDERMAL CORNIFICATION**

Received for publication, January 24, 2006, and in revised form, March 13, 2006 Published, JBC Papers in Press, March 24, 2006, DOI 10.1074/jbc.M600694200

Tsing Cheng[‡1], Kiyotaka Hitomi[§1], Ivonne M. J. J. van Vlijmen-Willems[‡], Gys J. de Jongh[‡], Kanae Yamamoto[§], Koji Nishi[§], Colin Watts[¶], Thomas Reinheckel[‖], Joost Schalkwijk[‡2], and Patrick L. J. M. Zeeuwen[‡]

From the [‡]Department of Dermatology, Nijmegen Centre for Molecular Life Sciences, Radboud University Nijmegen Medical Centre, P. O. Box 9101, 6500 HB Nijmegen, The Netherlands, the [§]Department of Applied Molecular Biosciences, Graduate School of Bioagricultural Sciences, Nagoya University, 464-8601 Nagoya, Japan, the [¶]Division of Cell Biology and Immunology, School of Life Sciences, University of Dundee, DD1 5EH Scotland, United Kingdom, and the [‖]Institute of Molecular Medicine and Cell Research, Albert-Ludwigs-University, D-79104 Freiburg, Germany

Cystatin M/E is a high affinity inhibitor of the asparaginyl endopeptidase legumain, and we have previously reported that both proteins are likely to be involved in the regulation of stratum corneum formation in skin. Although cystatin M/E contains a predicted binding site for papain-like cysteine proteases, no high affinity binding for any member of this family has been demonstrated so far. We report that human cathepsin V (CTSV) and human cathepsin L (CTSL) are strongly inhibited by human cystatin M/E. Kinetic studies show that K_i values of cystatin M/E for the interaction with CTSV and CTSL are 0.47 and 1.78 nM, respectively. On the basis of the analogous sites in cystatin C, we used site-directed mutagenesis to identify the binding sites of these proteases in cystatin M/E. We found that the W135A mutant was rendered inactive against CTSV and CTSL but retained legumain-inhibiting activity. Conversely, the N64A mutant lost legumain-inhibiting activity but remained active against the papain-like cysteine proteases. We conclude that legumain and papain-like cysteine proteases are inhibited by two distinct non-overlapping sites. Using immunohistochemistry on normal human skin, we found that cystatin M/E co-localizes with CTSV and CTSL. In addition, we show that CTSL is the elusive enzyme that processes and activates epidermal transglutaminase 3. The identification of CTSV and CTSL as novel targets for cystatin M/E, their (co)-expression in the stratum granulosum of human skin, and the activity of CTSL toward transglutaminase 3 strongly imply an important role for these enzymes in the differentiation process of human epidermis.

The cellular activity of a protease is the result of many regulatory mechanisms such as the concentration and compartmentalization of substrates, the enzyme itself, and its cognate inhibitors. Cystatins are the natural and specific inhibitors of endogenous mammalian lysosomal cysteine proteases and have shown important regulatory and protective functions in cells and tissues against proteolysis by cysteine proteases of host, bacterial, and viral origin (1–3). The inhibitory activity of cystatins is regulated by a reversible, tight-binding interaction between the protease inhibitor and its target protease (4). Disturbance of the normal balance between cysteine proteases and their inhibitors at a wrong time and location can lead to several pathological conditions such as chronic inflammatory reactions (5), tumor malignancy (6), and faulty differentiation processes in the epidermis and hair follicle (7). Little is known on the specific biological functions of cystatin family members. However, mutations in the genes encoding the cystatin family members cystatin B and C cause neurological phenotypes in humans (8, 9).

Cystatin M/E is a 14-kDa secreted protein that shares only 35% homology with other human type 2 cystatins. Nevertheless, it has a similar overall structure including the two characteristic intrachain disulfide bridges (10, 11). Expression of cystatin M/E is found to be restricted to the epidermis, more specifically in the stratum granulosum, sweat glands, sebaceous glands, and the hair follicles (12, 13). In addition to its function as a cysteine protease inhibitor, cystatin M/E also serves as a target for cross-linking by transglutaminases (12). These findings have suggested an important role for cystatin M/E in skin physiology. We have previously reported that a null mutation in the mouse cystatin M/E gene causes the murine *ichq* phenotype, which is characterized by neonatal lethality and abnormalities in cornification and desquamation, demonstrating an essential role for cystatin M/E in the final stages of epidermal differentiation (14). However, cystatin M/E was excluded as the causative gene in a lethal form of ichthyosis in humans (15). Recently, we proposed the involvement of the asparaginyl endopeptidase legumain in disturbed epidermal cornification in cystatin M/E-deficient mice (16). Legumain belongs to family C13 of cysteine proteases, which is unrelated to the family of papain-like cysteine proteases, and is strictly specific for hydrolysis of asparaginyl bonds (17). This lysosomal protease was shown to be involved in the processing of other lysosomal proteases such as cathepsins B, H, and L (18, 19). Furthermore, a biochemical study on legumain has indicated that cystatin M/E *in vitro* binds to this protease with high affinity (20). We have shown that cystatin M/E deficiency in mice leads to free cutaneous legumain activity, increased transepidermal water loss, and dehydration. We have reported that disturbed cornification is caused by abnormalities in loricrin processing, which may be the result of abnormal activation of

* This work was supported by a grant from the Radboud University Nijmegen Medical Centre (to T. C.) and by VENI-Grant 916.56.117 from ZONMW, the Netherlands Organization for Health Research and Development (to P. L. J. M. Z.). The costs of publication of this article were defrayed in part by the payment of page charges. This article must therefore be hereby marked "*advertisement*" in accordance with 18 U.S.C. Section 1734 solely to indicate this fact.

[1] Both authors contributed equally to this study.

[2] To whom correspondence should be addressed. Tel.: 31-24-3614094; Fax: 31-24-3541184; E-mail: j.schalkwijk@derma.umcn.nl.

transglutaminase 3 (TGase 3)[3] by cathepsins, whose activities in their turn could be regulated by legumain (16). During keratinocyte differentiation, TGase 3 is activated by limited proteolysis of a 77-kDa zymogen (21, 22), a process that is apparently under control of cystatin M/E, at least during skin morphogenesis in the neonatal phase. These data suggest that cystatin M/E plays a key role in the regulation of proteolytic events that are involved in barrier formation and maintenance. To understand this process in more detail at the molecular and cellular level, we set out to identify the relevant enzymes and inhibitors and to study their localization in human skin. The identification of CTSV and CTSL as novel targets for cystatin M/E, their expression in human skin, and the processing activity of CTSL toward TGase 3 strongly imply an important role for these enzymes in the differentiation process of human epidermis.

EXPERIMENTAL PROCEDURES

Three-dimensional Modeling of Cystatin M/E—A three-dimensional model of human cystatin M/E was generated using MODELLER (23). The crystal structure of human cystatin D (Protein Data Bank identification number 1Roa) was used as a starting point. Human cystatin D and cystatin M/E have a 26% sequence identity. The sequences were aligned using the internal aligner of MODELLER; this routine uses a gap function that depends on the secondary structure.

Production of Cystatin M/E Variants—Cystatin M/E variants N64A and W135A were obtained using the recombinant plasmid pGEX-2T/cystatin M/E (a kind gift of Dr Georgia Sotiropoulou) and QuikChange site-directed mutagenesis kit (Stratagene, La Jolla, CA). Primers used for the generation of the N64A variant were 5′-GCTACAACATGGGCAGCGCCAGCATCTACTACTTCC-3′ (sense) and 5′-GGAAGTAGTAGATGCTGGCGCTGCCCATGTTGTAGC-3′ (antisense). Primers for the W135A variant were 5′-GGTCCTTGTGGTTCCCGCGCAGAACTCCTCTCAGC (sense) and 5′-GCTGAGAGGAGTTCTGCGCGGGAACCACAAGGACC-3′ (antisense). All primers were from Biolegio (Malden, The Netherlands). Sequence analysis was performed to check for the desired mutations in the cDNA.

Production of Recombinant Proteins—Production and purification of recombinant wild type and mutant forms of human cystatin M/E were performed as described previously (10) with minor changes. pGEX-2T plasmids containing the wild type or mutated cystatin M/E cDNAs were transformed into *Escherichia coli* BL21 Star (DE3) bacteria (Invitrogen). Cultures were grown from one single colony overnight at 37 °C in LB medium with ampicillin followed by induction with isopropyl-1-thio-β-D-galactopyranoside (Roche Applied Science) at a final concentration of 0.5 mM for 2 h at 37 °C. Cells were lysed by four cycles of freezing in liquid nitrogen and thawing. Glutathione-Sepharose 4B beads (Amersham Biosciences) were used for purification of glutathione *S*-transferase fusion protein from the lysate. Cleavage of the fusion protein into glutathione *S*-transferase and cystatin M/E occurred overnight at 4 °C with thrombin (Sigma) at a thrombin to fusion protein ratio of 1:500 in a buffer containing 50 mM Tris-HCl (pH 7.5), 150 mM NaCl, and 2.5 mM $CaCl_2$. Recombinant cystatin M/E was purified from glutathione *S*-transferase using glutathione-Sepharose 4B beads and dialyzed against phosphate-buffered saline with an YM3 filter (Millipore, Billerica, MA). Protein concentration was determined using a BCA protein assay (Pierce).

Fluorimetric Enzyme Assays—Protease inhibitory activity of recombinant human wild type cystatin M/E, the N64A and W135A variants, and the recombinant human cystatins A, B, C, D, F, and S (all from R&D Systems, Minneapolis, MN) against recombinant human legumain (24), human CTSV (R&D Systems), and human CTSL (one-chain form, recombinant protein, R&D Systems; two-chain form, purified from human liver, Sigma) was determined by measuring inhibition of the proteases using the fluorogenic synthetic substrates Z-Ala-Ala-Asn-MCA (4-methyl-coumaryl-7-amide) (Peptides International, Louisville, KY) for legumain and Z-Leu-Arg-AMC (7-amino-4-methyl-coumarin) (R&D Systems) for CTSV and CTSL. Protease inhibition was measured after an incubation period of 5 min (CTSL) or 10 min (legumain, CTSV) at room temperature. The buffer that was used in the legumain assay contained 0.1 M phosphate (pH 5.7), 2 mM EDTA, 1 mM dithiothreitol, 2.67 mM L-cysteine, and 100 μg/μl bovine serum albumin. CTSV and CTSL assays were performed in buffer (pH 5.5) containing 0.1 M acetate, 1 mM EDTA, 2 mM dithiothreitol, and 100 μg/μl bovine serum albumin. Reactions were stopped by adding 0.1 M Na_2CO_3 (pH 8.5). K_i values were determined using the Easson-Stedman plot as described by Bieth (25) and as indicated in the legend of Fig. 2.

Immunohistochemistry—Human skin biopsies were processed for immunohistochemistry as described previously (13, 26). Immunohistochemical staining was performed according to the avidin biotinylated-enzyme-complex method (Vector, Burlingame, CA) using polyclonal rabbit-anti-human cystatin M/E antibodies (12), polyclonal sheep-anti-human legumain antibodies (24), monoclonal mouse-anti-human CTSV antibodies (R&D Systems), and monoclonal rat-anti-human/mouse CTSL antibodies (R&D Systems).

Digestion of TGase 3 Zymogen with Cathepsins—Baculovirus expressed recombinant human TGase 3 zymogen (22) was processed by treatment with recombinant human CTSL, CTSV, cathepsin B (CTSB), cathepsin S (CTSS), and cathepsin D (CTSD) (all from R&D Systems). To prepare the proteolyzed form of TGase 3, 4 μg of zymogen was treated with cathepsins using a molar ratio of ~0.001: CTSL (2.8 ng), CTSV (2 ng), CTSS (2 ng), and CTSB (1.9 ng). In the case of CTSD, the ratio is about 0.05 (80 ng). Each incubation was performed in the appropriate buffers as follows: for CTSL, CTSV, CTSB, and CTSS, 100 mM MES (pH 6.0), 16 mM dithiothreitol, 1.6 mM EDTA; and for CTSD, 100 mM sodium acetate (pH 4.0), 100 mM KCl. For controls, the same reaction mixtures were prepared but with the addition of pepstatin (Nacarai, Kyoto, Japan), which is an inhibitor of the aspartic protease CSTD, or E-64 (*trans*-epoxysuccinyl-L-leucylamido-(4-guanidino)butane, Peptide Institute Inc., Osaka, Japan), a synthetic inhibitor of the cysteine proteases CTSL, CTSV, CTSB, and CTSS. Both controls were used at a final concentration of 10 μM. Reactions were performed at 37 °C for the indicated times (see Fig. 4).

Immunoblotting—Reaction mixtures with proteolyzed TGase 3 were subjected to SDS-PAGE and electroblotted onto polyvinylidene difluoride membrane as described previously (27). The membrane was incubated with anti-human TGase 3 monoclonal antibodies C2D and C9D, which specifically recognize the zymogen form and the proteolyzed 30- and 47-kDa fragments, respectively (27). Detection of the proteins was established with peroxidase-conjugated anti-mouse IgG and IgM (Jackson ImmunoResearch Laboratories, West Grove, PA) and SuperSignal West Pico chemiluminescent substrate (Pierce) according to the manufacturer's protocol.

TGase 3 Activity—Prior to the assay, E-64 was added to the reaction mixture to block cathepsin activity. TGase 3 activity was measured by a 96-well plate assay as described previously (28, 29). Briefly, 1% dimethylcasein was fixed at the plate, and the uncoated sites were blocked with skimmed milk. The sample was incubated with 5-(biotinamido-)pentylamine (Pierce) in a buffer containing 100 mM Tris-HCl (pH 8.0), 10 mM

[3] The abbreviations used are: TGase, transglutaminase; CTSV, cathepsin V; CTSL, cathepsin L; CTSB, cathepsin B; CTSS, cathepsin S; CTSD, cathepsin D; MES, 2-(N-morpholino)ethanesulfonic acid; E-64, *trans*-epoxysuccinyl-L-leucylamido-(4-guanidino)butane; Z, benzyloxycarbonyl.

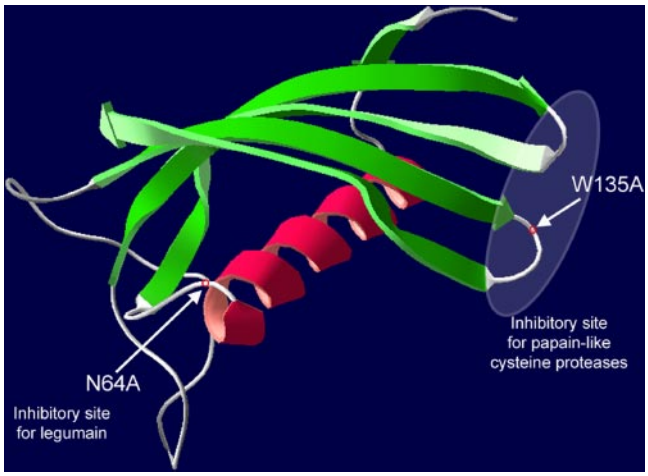

FIGURE 1. **Predicted three-dimensional representation of cystatin M/E.** The crystal structure of cystatin D was used as a basis for this model. The regions of the inhibitory sites for papain-like cysteine proteases and for legumain are marked. The locations of the amino acids substituted in the cystatin M/E variants are shown in *white*.

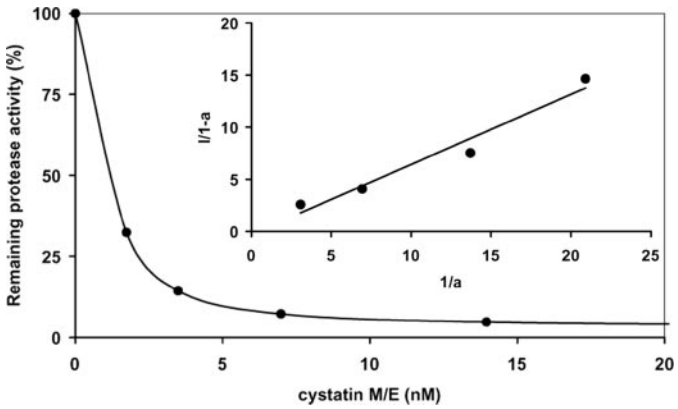

FIGURE 2. **Determination of the dissociation constant K_i of the protease/protease-inhibitor complex.** The dissociation constant K_i was determined by measuring the residual enzymatic activity of a fixed concentration of enzyme (as shown here for CTSV) incubated with increasing concentrations of inhibitor (cystatin M/E). An Easson-Stedman plot (*inset*) was used to calculate the K_i. The *inset* is a replot of the data according to the following equation: $[I]/1 - a = (K_i/a) + E^0$, where I is the inhibitor concentration, E^0 the enzyme concentration at time 0, and a is the fractional activity, *i.e.* the ratio between the enzyme activity in the presence (V_i) and absence (V_0) of the inhibitor. The plot yields a straight line whose slope is K_i. A representative curve of three experiments is shown.

dithiothreitol, and 5 mM $CaCl_2$. After various periods of incubation, the reaction was blocked by adding EDTA at a final concentration of 10 mM. TGase-catalyzed conjugation of 5-(biotinamido-)pentylamine to dimethylcasein was measured by avidin-conjugated peroxidase, hydrogen peroxide, *o*-phenylenediamine, and hydroxy peroxide. An equal volume of 2 M H_2SO_4 was added, and the absorbance was measured at 450 nm.

Determination of the TGase 3 Cleavage Site—Ten micrograms of human TGase 3 was digested with 10 ng of CTSL, and the resulting fragments were subjected to SDS-PAGE, blotted onto polyvinylidene difluoride membrane, and subsequently stained with Coomassie Blue. The N-terminal amino acid sequence of the 30-kDa fragment was determined by automated Edman degradation.

RESULTS

Inhibition of Protease Activity by Cystatin M/E—Based on the homology with cystatin C, we predicted that cystatin M/E would contain two distinct binding sites for papain-like cysteine proteases and for the asparaginyl endopeptidase legumain. A three-dimensional model of human cystatin M/E was generated on the basis of the published crystal structure of human

TABLE 1

K_i values of wild type cystatin M/E and mutated variants for legumain, cathepsin V, and cathepsin L

Cystatin M/E	K_i legumain	K_i cathepsin V	K_i cathepsin L
	nM	nM	nM
Wild type	0.25	0.47	1.78
N64A	>100[a]	0.34	1.77
W135A	0.72	>100[b]	11.7

[a] $v_i/v_0 > 0.60$ at [I] = 100 nM.
[b] $v_i/v_0 > 0.50$ at [I] = 100 nM.

TABLE 2

K_i values of human cystatins for legumain, cathepsin V, and cathepsin L

Cystatin	K_i legumain	K_i cathepsin V	K_i cathepsin L
	nM	nM	nM
cystatin A	>100[a]	0.11	0.05
cystatin B	>100[a]	0.13	0.05
cystatin C	7.28	0.02	0.08
cystatin D	>100[a]	29.6	2.81
cystatin F	>100[a]	>100[b]	0.49
cystatin S	>100[a]	>100[c]	>100[d]

[a] $v_i/v_0 > 0.99$ at [I] = 100 nM.
[b] $v_i/v_0 > 0.70$ at [I] = 100 nM.
[c] $v_i/v_0 > 0.90$ at [I] = 100 nM.
[d] $v_i/v_0 > 0.85$ at [I] = 100 nM.

cystatin D (30), which revealed that the overall predicted structure of cystatin M/E closely matched that of cystatin D (Fig. 1). To study the presumed reactive sites and the inhibitory activities of cystatin M/E, variants of the protein with an inactive site for either legumain or papain-like cysteine proteases were generated by substitution of one of the conserved amino acids. As shown in Fig. 1, the N64A variant has a substitution of the Asn^{64} residue of the proposed legumain inhibitory site by an Ala residue, whereas the W135A variant has its Trp^{135} residue of the papain-like cysteine protease inhibitory site substituted by an Ala residue. Wild type and mutant cystatin M/E was tested for inhibitory activity against legumain and several papain-like cysteine proteases. In previous studies, it was found that cystatin M/E was a poor inhibitor of most lysosomal cathepsins. Here we extended our studies to include CTSV and we also included the one-chain form of CTSL, as this form is the one expressed in skin. K_i values were determined using an Easson-Stedman plot as illustrated in Fig. 2 for CTSV and wild type cystatin M/E. When the K_i could not be determined in the case of very low affinity, the ratio of protease activity in the presence (V_i) and absence (V_0) of inhibitor was determined, and the remaining protease activity at a fixed high inhibitor concentration was calculated. K_i values of wild type human cystatin M/E and the N64A and W135A variants for interaction with human legumain and the human cysteine proteases CTSV and CTSL are shown in Table 1. Wild type cystatin M/E is a high affinity inhibitor for legumain, CTSV, and CTSL as witnessed by their respective K_i values of 0.25, 0.47, and 1.78 nM. Similar K_i values were found for interaction of the N64A variant with CTSV and CSTL but not with legumain ($V_i/V_0 > 0.60$ at [I] = 100 nM). The K_i value of the W135A variant for interaction with legumain was in the same range as that of wild type cystatin M/E, whereas the K_i value for interaction with CTSV could not be determined ($V_i/V_0 > 0.50$ at [I] = 100 nM). The W135A mutation did not decrease the affinity for CTSL at a similar order of magnitude as for CTSV but still caused a 6-fold increase of the K_i value as compared with that of wild type cystatin M/E (11.7 nM *versus* 1.78 nM). Similar experiments with several other human cystatins were performed and K_i values for the interaction with human legumain, CTSV, and CTSL are shown in Table 2. CTSV was efficiently inhibited by cystatins A, B, and C (K_i values below 0.15 nM),

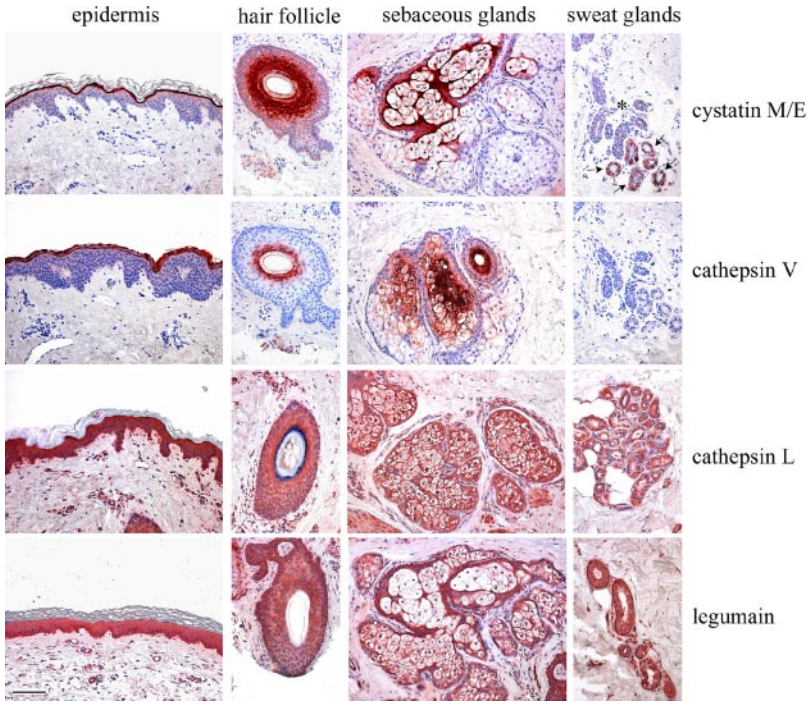

FIGURE 3. **Immunostaining for cystatin M/E, cathepsin V, cathepsin L, and legumain in normal human skin and its appendages.** Note the stratum-specific expression of cystatin M/E and CTSV in the stratum granulosum of the epidermis. CTSV is only present in the inner layer of the outer root sheet of the hair follicle, whereas cystatin M/E is also expressed in many more layers of the outer root sheet of the hair follicle. The secretory coil epithelium of the sweat glands is positively stained for cystatin M/E (*arrowheads*), but the ductal part is almost negative (the *asterisk* is surrounded by ducts). No expression of CTSV was found in the sweat glands. CTSL and legumain are also expressed in the stratum granulosum. Furthermore, positive staining was also found in the other layers of the epidermis and its appendages. The sweat gland ducts as well as the secretory coils are both positively stained for CTSL and legumain. *Scale bar* = 100 μm.

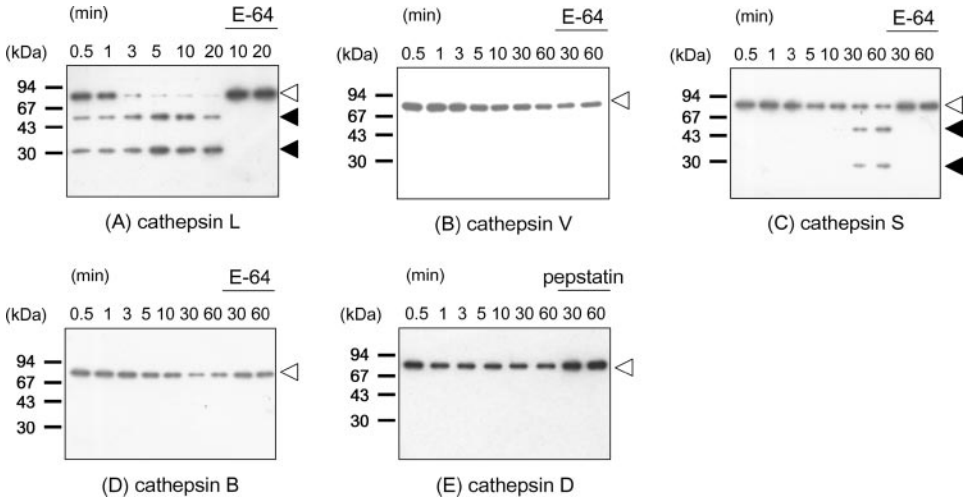

FIGURE 4. **Proteolysis of human TGase 3 by cathepsins.** Four micrograms of recombinant human TGase 3 was treated with several cathepsins at 37 °C for the indicated times. The reaction mixtures were subjected to SDS-PAGE followed by immunoblotting analysis using monoclonal antibodies C2D and C9D. Reactions were also performed in the presence of specific inhibitors (E-64 or pepstatin) at a final concentration of 10 μM. The 77-kDa TGase 3 zymogen is rapidly proteolyzed into its 30- and 47-kDa fragments by CTSL (*A*) but not by CTSV (*B*), CTSS (*C*), CTSB (*D*), and CTSD (*E*). The *open* and *closed arrowheads* indicate zymogen and proteolyzed TGase 3, respectively.

whereas the affinity of CTSV for cystatin D was weaker (K_i of 29.6 nM) and not detectable with cystatins F and S. CTSL was efficiently inhibited by cystatins A, B, C, and F (K_i values below 0.5 nM), whereas the affinity for cystatin D was somewhat weaker (K_i of 2.81 nM). Cystatin S showed no inhibition with any of the tested cysteine proteases, whereas the ubiquitously expressed cystatin C demonstrated strong inhibitory activity for all of them, although its affinity for legumain is much weaker than that of cystatin M/E (7.28 nM *versus* 0.25 nM).

Co-expression of Cystatin M/E and Its Biological Targets in the Stratum Granulosum—To establish a functional link between cystatin M/E and its putative target proteases, we investigated their expression at the tissue level in human skin. Immunohistochemistry was performed on skin biopsies from healthy volunteers. In normal human skin, cystatin M/E and CTSV are strongly and specifically expressed in the stratum granulosum of the epidermis (Fig. 3). In addition, both proteins are also expressed in the hair follicle. CTSV is only present in a small layer of the hair follicle root sheet, whereas cystatin M/E is expressed throughout the inner half of the root sheet. The sweat glands showed no expression of CTSV, whereas the secretory coil epithelium but not the ductal part of the sweat glands was positive for cystatin M/E. CTSV and cystatin M/E both show a positive staining in the inner, mature cells of the sebaceous glands. In contrast to cystatin M/E and CTSV, the expression of legumain and CTSL was not limited to a specific cell layer but was found throughout all layers of the epidermis and its appendages (Fig. 3).

Activation of TGase 3 by CTSL—In a previous study, we have found that lysosomal cysteine proteases are probably involved in the processing of human epidermal TGase 3 *in vitro*, suggesting that this could be a mechanism for activation. So far, the responsible proteases for this activation remained unknown. To address this issue more in depth at the functional level, recombinant human TGase 3 was incubated with a panel of recombinant human lysosomal cysteine proteases to investigate their proteolytic activity toward the zymogen form of TGase 3. We found that CTSL is able to proteolyze TGase 3 into 30- and 47-kDa fragments (Fig. 4*A*) in a concentration- and time-dependent manner. When the cathepsin inhibitor E-64 was added to the reaction mixture, no TGase 3 proteolysis could be detected. Other cathepsins were not

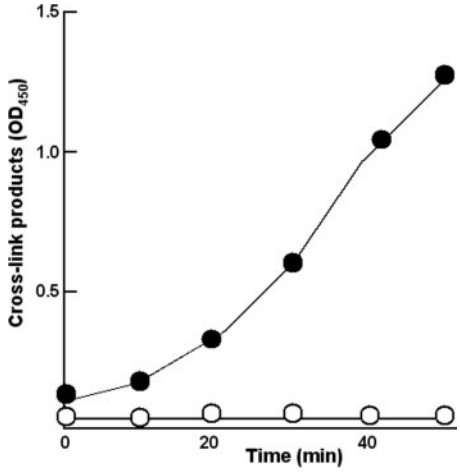

FIGURE 5. **Activity of TGase 3 proteolyzed by cathepsin L.** The enzymatic activity of proteolyzed TGase 3 was measured after digestion with CTSL for 3 min. The enzymatic reaction products are shown as the value of $A_{450\ nm}$. The *open* and *closed circles* indicate the reactions using 100 ng of zymogen and the proteolyzed forms, respectively.

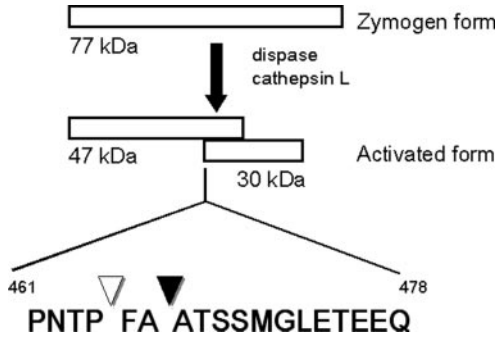

FIGURE 6. **Processing of TGase 3.** The 77-kDa zymogen form of TGase 3 is proteolyzed into the activated form consisting of 30- and 47-kDa fragments, which then associate non-covalently to form the active enzyme (21). The N-terminal sequence of the 30-kDa fragment of human TGase 3 was determined by automated Edman degradation. For comparison, we show the cleavage site of TGase 3 after digestion by dispase, a neutral bacterial protease that is commonly used to activate TGase 3 *in vitro*. The *open* and *closed triangles* represent the cleavage sites of dispase and CTSL digestion, respectively.

able to cleave the TGase 3 zymogen in this experimental setup (Fig. 4, *B–E*), except in the case of longer incubation times with cathepsin S (Fig. 4*C*). In the presence of relatively high amounts of cathepsins B, S, and V in the reaction mixture (molar ratio of 1:10), TGase 3 was limitedly proteolyzed (data not shown). Next, we measured the enzymatic activity of the proteolyzed products of TGase 3 zymogen that was digested by CTSL. Although the TGase 3 zymogen showed no enzymatic activity, TGase proteolyzed by the action of CTSL demonstrated an apparent enzymatic activity (Fig. 5). N-terminal sequencing of the 30-kDa TGase 3 fragment revealed that the CTSL cleavage site in TGase 3 is before Ala^{467}, two amino acids downstream as compared with the cleavage site generated by dispase digestion (Fig. 6).

DISCUSSION

In this study, we show that the protease inhibitor cystatin M/E inhibits legumain and papain-like cysteine proteases due to two distinct non-overlapping sites. The papain-like cysteine proteases CTSV and CTSL are strongly inhibited by cystatin M/E, suggesting that these proteases are new targets for cystatin M/E. Immunostaining of cystatin M/E, CTSV, CTSL, and legumain in normal human skin shows co-expression, especially in the stratum granulosum and the hair follicles, suggesting that these enzymes have an important role in human epidermal differentiation and hair follicle morphogenesis. Our data indicate that CTSL is the elusive protease that can process and activate TGase 3, an enzyme that is involved in cornified envelope formation.

Based on the homology with cystatin D, we generated a three-dimensional model of cystatin M/E. This model shows that a loop located on the opposite side to the cysteine protease-binding surface, between the α-helix and the first strand of the main β-sheet of the cystatin M/E structure, contains the asparaginyl residue that is probably involved in legumain binding. Site-directed mutagenesis was used to identify the presumed binding sites of papain-like cysteine proteases and that of the asparaginyl endopeptidase legumain in cystatin M/E. Substitution of a conserved amino acid by alanine in the two reactive sites resulted in loss of inhibitory activity. We could confirm that the conserved Asn^{64} residue (cystatin M/E numbering) in the legumain inhibitory site is important for cystatin-legumain interaction. Our K_i values for this interaction are somewhat higher than the K_i values found by Alvarez-Fernandez *et al.* (20), but this could be explained by our use of recombinant human legumain, whereas pig legumain extracted from kidney was used by the group of Alvarez-Fernandez. Cystatins are known as inhibitors of lysosomal cysteine proteases of the papain family (C1). Although cystatin M/E contains a predicted binding site for papain-like cysteine proteases, no high affinity binding for any member of this family had been demonstrated so far (11, 12, 16). The present study shows that cystatin M/E is a high affinity inhibitor of CTSV and CTSL. For this study, we used recombinant CTSL that was obtained as a one-chain form, which is the relevant form for skin (31). In general, CTSL is translated as prepro-CTSL, and during intracellular transport to the lysosomes, the preproenzyme is subsequently modified to pro-CTSL and processed into the mature one-chain and two-chain forms of CTSL. Processing of pro-CTSL results in a ~30-kDa one-chain form of CTSL, which in turn can be further processed into the two-chain form (5 and 24 kDa) (32). It is not known whether this conversion regulates CTSL activity or substrate specificity, but recently, it has been reported that both forms are proteolytically active and can execute the essential functions of CTSL (19, 32). As we had previously found that CTSL purified from human liver (the two-chain form) was only weakly inhibited by cystatin M/E, the strong inhibition by recombinant one-chain form CTSL was unexpected. Comparison of human liver CTSL from different suppliers revealed that we have previously underestimated the inhibition of cystatin M/E for reasons we cannot explain. Based on the CTSL preparations used in this study both the one-chain and two-chain form of CTSL are inhibited equally well by cystatin M/E (not shown). CTSV is a recently discovered protease, also known as cathepsin L2 or stratum corneum thiol protease. CTSV is closely related to CTSL sharing ~80% protein sequence identity (33–36). Their encoding genes are located on adjacent sites on chromosome 9q22.2, suggesting that CTSV and CTSL have evolved by duplication from an ancestral gene (35). However, although CTSL is ubiquitously expressed, CTSV expression is more restricted and predominantly found in thymus, testis, cornea of the eye, and epidermis (33, 34, 36). Besides the general function of lysosomal cathepsins, *i.e.* bulk proteolysis, studies using a knock-out mouse model have suggested that CTSL has specific functions in keratinocyte proliferation and hair follicle morphogenesis and cycling (37–39).

The role of CTSV and CTSL in terminal differentiation of keratinocytes and hair follicle morphogenesis is unknown, but these proteins probably process and activate other enzymes in pathways that lead to skin barrier formation. Our biochemical assays show that CTSL is the first identified mammalian protease that is able to cleave and activate TGase 3 *in vitro* (Figs. 4 and 5). TGase 3 is an epidermis-specific enzyme responsible for cross-linking loricrin and small proline-rich proteins in the stratum granulosum (27, 40). TGase 3 is also the most efficient

cross-linking enzyme of soluble trichohyalin, a major structural protein in hair follicle differentiation (41). Remarkably, a reduced expression of trichohyalin was found in CTSL-deficient mice (38). Our results provide evidence that CTSL initiates the cross-linking activity of TGase 3 in the process that leads to cornification, by cleavage of the 77-kDa TGase 3 zymogen and thereby activation of the enzyme. This mechanism could possibly be regulated by the inhibitory activity of cystatin M/E against CTSL. Legumain inhibition by cystatin M/E could have a regulatory role in CTSL activity since legumain is involved in CTSL processing (18, 19). Cystatin M/E-deficient mice show epidermal and follicular hyperkeratosis resulting in a scaly skin, abnormal hair follicles, and an impaired barrier function (14). This could be explained by elevated CTSL and/or legumain activities due to cystatin M/E deficiency that subsequently lead to an early or excessive activation of TGase 3, resulting in a premature or enhanced cross-linking of loricrin molecules and small proline-rich proteins, incomplete desquamation, thickening of the stratum corneum, and abnormal hair morphogenesis.

N-terminal sequencing of the 30-kDa fragment revealed that CTSL cleaves TGase 3 between amino acids Ala^{466} and Ala^{467} (Fig. 6). TGase 3, as well as other TGases, consists of four domains: a β-sandwich, a catalytic core, β-barrel-1, and β-barrel-2. In TGase 3, the unique hinge region (Pro^{461}–Glu^{479}) separates the catalytic core and β-barrel-1 domain (21). In our previous studies, the cleavage site of human TGase 3 by dispase-digestion was Phe^{465}, which is located in this hinge region (42). Since treatment of TGase 3 with thrombin or trypsin produces 30- and 47-kDa fragments, this hinge region appears to be a domain that is sensitive to proteolysis (43). As CTSL preferentially cleaves peptide bonds with aromatic residues in P2 and hydrophobic residues in the P3 position (44), we believe that we have identified the exact cleavage site of human TGase 3 by CTLS. This conclusion is based on the fact that in the P2 and P3 position of the TGase 3 cleavage site, an aromatic residue (Phe^{465}) and a hydrophobic residue (Pro^{464}) are found, respectively. Future studies should clarify whether this is the physiological cleavage site *in vivo* as well.

It is likely that CTSV has a role in skin that is distinct from CTSL because its expression is specifically restricted to the upper epidermal layers. The secretion of both cystatin M/E and CTSV by differentiating keratinocytes (12, 36) makes them both plausible candidates to be involved in desquamation. A detailed description of the cellular and subcellular localization of cystatin M/E and its target proteases in epidermis and hair follicles was beyond the scope of this report. Our immunohistochemical data comprise only a small part of the human hair follicle, and the transverse sections at the level of the infundibulum (Fig. 3) preclude a detailed analysis of the inner and outer root sheet at the deeper levels.

Biochemical enzyme assays with cystatins other than cystatin M/E show that cystatins A, B, and C are strong inhibitors of CTSV and CTSL as well. Cystatin A is known to be expressed in skin and participates in epidermal barrier formation and function (45, 46). Cystatin A belongs to the type 1 cystatins, which are primarily intracellular proteins. Cystatin M/E on the other hand can be secreted, probably into the extracellular space between corneocytes. Keeping this in mind, it is possible that CTSV and/or CTSL activity in the upper epidermal layers of the skin is intracellularly regulated by cystatin A and extracellularly regulated by cystatin M/E. Compartmentalization studies at the ultrastructural level could shed further light on the exact role of cystatin M/E and its protease targets.

Recently, the phenotype of CTSL knock-out mice was rescued by transgenic epidermal re-expression of either murine CTSL or human CTSV, indicating that human CTSV can compensate for murine CTSL (47, 48). No orthologue of CTSV in mice has been discovered yet, but it is plausible that murine CTSL is actually the orthologue of human CTSV, in view of the fact that human CTSV is phylogenetically more closely related to murine CTSL than to human CTSL (47). Our immunohistochemical data provide a novel clue in support of this theory since in epidermis, CTSV expression in the upper epidermal layers is similar to that of murine CTSL. Another possibility is that murine CTSL controls the specific functional enzymatic activities of both human CTSL and CTSV. A closer inspection of hair follicle morphogenesis in CTSL-deficient mice showed that defects in the differentiation, keratinization, and desquamation of the inner root sheet form the basis of the abnormal hair phenotype (38). Therefore, a more in-depth study of cellular and subcellular localization of CTSL and TGase 3 in the entire human hair follicle is required to elucidate the potential role of these molecules in hair follicle morphogenesis.

We conclude that cystatin M/E has an important regulatory function in human epidermal differentiation. Cystatin M/E could regulate cross-linking of structural proteins by TGase 3 in cornified envelope formation through inhibitory activities against CTSL and legumain. In addition, cystatin M/E could also have a role in the desquamation process as CTSV activity is involved in the degradation of corneodesmosomes. Further studies are necessary to elucidate the regulatory role of cystatin M/E in pathways that are involved in desquamation. CTSV and CTSL may activate other transglutaminases such as TGase 1 and TGase 5, or other proteases, such as cathepsin D, that are involved in terminal differentiation. Recently, it has been demonstrated that cathepsin D-deficient mice show a reduced TGase 1 activity and impaired stratum corneum morphology, similar to the skin of TGase 1 knock-out mice and the human skin disease lamellar ichthyosis (49). Collectively, this finding and the data from our studies strongly support a functional link between protease activity and activation of TGases in the epidermis.

REFERENCES

1. Abrahamson, M., Alvarez-Fernandez, M., and Nathanson, C. M. (2003) *Biochem. Soc. Symp.* 179–199
2. Bobek, L. A., and Levine, M. J. (1992) *Crit. Rev. Oral Biol. Med.* **3,** 307–332
3. Turk, B., Turk, V., and Turk, D. (1997) *Biol. Chem.* **378,** 141–150
4. Turk, B., Turk, D., and Salvesen, G. S. (2002) *Curr. Pharm. Des.* **8,** 1623–1637
5. Henskens, Y. M., Veerman, E. C., and Nieuw Amerongen, A. V. (1996) *Biol. Chem. Hoppe-Seyler* **377,** 71–86
6. Calkins, C. C., and Sloane, B. F. (1995) *Biol. Chem. Hoppe-Seyler* **376,** 71–80
7. Zeeuwen, P. L. (2004) *Eur. J. Cell Biol.* **83,** 761–773
8. Pennacchio, L. A., Lehesjoki, A. E., Stone, N. E., Willour, V. L., Virtaneva, K., Miao, J., D'Amato, E., Ramirez, L., Faham, M., Koskiniemi, M., Warrington, J. A., Norio, R., de la, C. A., Cox, D. R., and Myers, R. M. (1996) *Science* **271,** 1731–1734
9. Palsdottir, A., Abrahamson, M., Thorsteinsson, L., Arnason, A., Olafsson, I., Grubb, A., and Jensson, O. (1988) *Lancet* **2,** 603–604
10. Sotiropoulou, G., Anisowicz, A., and Sager, R. (1997) *J. Biol. Chem.* **272,** 903–910
11. Ni, J., Abrahamson, M., Zhang, M., Fernandez, M. A., Grubb, A., Su, J., Yu, G. L., Li, Y., Parmelee, D., Xing, L., Coleman, T. A., Gentz, S., Thotakura, R., Nguyen, N., Hesselberg, M., and Gentz, R. (1997) *J. Biol. Chem.* **272,** 10853–10858
12. Zeeuwen, P. L., van Vlijmen-Willems, I. M., Jansen, B. J., Sotiropoulou, G., Curfs, J. H., Meis, J. F., Janssen, J. J., van, R. F., and Schalkwijk, J. (2001) *J. Investig. Dermatol.* **116,** 693–701
13. Zeeuwen, P. L., van Vlijmen-Willems, I. M., Egami, H., and Schalkwijk, J. (2002) *Br. J. Dermatol.* **147,** 87–94
14. Zeeuwen, P. L., van Vlijmen-Willems, I. M., Hendriks, W., Merkx, G. F., and Schalkwijk, J. (2002) *Hum. Mol. Genet.* **11,** 2867–2875
15. Zeeuwen, P. L., Dale, B. A., de Jongh, G. J., van Vlijmen-Willems, I. M., Fleckman, P., Kimball, J. R., Stephens, K., and Schalkwijk, J. (2003) *J. Investig. Dermatol.* **121,** 65–68
16. Zeeuwen, P. L., van Vlijmen-Willems, I. M., Olthuis, D., Johansen, H. T., Hitomi, K., Hara-Nishimura, I., Powers, J. C., James, K. E., op den Camp, H. J., Lemmens, R., and Schalkwijk, J. (2004) *Hum. Mol. Genet.* **13,** 1069–1079
17. Chen, J. M., Dando, P. M., Rawlings, N. D., Brown, M. A., Young, N. E., Stevens, R. A., Hewitt, E., Watts, C., and Barrett, A. J. (1997) *J. Biol. Chem.* **272,** 8090–8098
18. Shirahama-Noda, K., Yamamoto, A., Sugihara, K., Hashimoto, N., Asano, M., Nishimura, M., and Hara-Nishimura, I. (2003) *J. Biol. Chem.* **278,** 33194–33199
19. Maehr, R., Hang, H. C., Mintern, J. D., Kim, Y. M., Cuvillier, A., Nishimura, M.,

Yamada, K., Shirahama-Noda, K., Hara-Nishimura, I., and Ploegh, H. L. (2005) *J. Immunol.* **174,** 7066–7074
20. Alvarez-Fernandez, M., Barrett, A. J., Gerhartz, B., Dando, P. M., Ni, J., and Abrahamson, M. (1999) *J. Biol. Chem.* **274,** 19195–19203
21. Ahvazi, B., Kim, H. C., Kee, S. H., Nemes, Z., and Steinert, P. M. (2002) *EMBO J.* **21,** 2055–2067
22. Hitomi, K., Kanehiro, S., Ikura, K., and Maki, M. (1999) *J. Biochem.* (*Tokyo*) **125,** 1048–1054
23. Sali, A., and Blundell, T. L. (1993) *J. Mol. Biol.* **234,** 779–815
24. Li, D. N., Matthews, S. P., Antoniou, A. N., Mazzeo, D., and Watts, C. (2003) *J. Biol. Chem.* **278,** 38980–38990
25. Bieth, J. G. (1980) *Bull. Eur. Physiopathol. Respir.* **16,** (suppl.) 183–197
26. El Ghalbzouri, A., Lamme, E., and Ponec, M. (2002) *Cell Tissue Res.* **310,** 189–199
27. Hitomi, K., Presland, R. B., Nakayama, T., Fleckman, P., Dale, B. A., and Maki, M. (2003) *J. Dermatol. Sci.* **32,** 95–103
28. Slaughter, T. F., Achyuthan, K. E., Lai, T. S., and Greenberg, C. S. (1992) *Anal. Biochem.* **205,** 166–171
29. Hitomi, K., Yamagiwa, Y., Ikura, K., Yamanishi, K., and Maki, M. (2000) *Biosci. Biotechnol. Biochem.* **64,** 2128–2137
30. Alvarez-Fernandez, M., Liang, Y. H., Abrahamson, M., and Su, X. D. (2005) *J. Biol. Chem.* **280,** 18221–18228
31. Ishidoh, K., Saido, T. C., Kawashima, S., Hirose, M., Watanabe, S., Sato, N., and Kominami, E. (1998) *Biochem. Biophys. Res. Commun.* **252,** 202–207
32. Ishidoh, K., and Kominami, E. (2002) *Biol. Chem.* **383,** 1827–1831
33. Adachi, W., Kawamoto, S., Ohno, I., Nishida, K., Kinoshita, S., Matsubara, K., and Okubo, K. (1998) *Investig. Ophthalmol. Vis. Sci.* **39,** 1789–1796
34. Santamaria, I., Velasco, G., Cazorla, M., Fueyo, A., Campo, E., and Lopez-Otin, C. (1998) *Cancer Res.* **58,** 1624–1630
35. Brömme, D., Li, Z., Barnes, M., and Mehler, E. (1999) *Biochemistry* **38,** 2377–2385
36. Watkinson, A. (1999) *Arch. Dermatol. Res.* **291,** 260–268
37. Roth, W., Deussing, J., Botchkarev, V. A., Pauly-Evers, M., Saftig, P., Hafner, A., Schmidt, P., Schmahl, W., Scherer, J., Anton-Lamprecht, I., Von Figura, K., Paus, R., and Peters, C. (2000) *FASEB J.* **14,** 2075–2086
38. Tobin, D. J., Foitzik, K., Reinheckel, T., Mecklenburg, L., Botchkarev, V. A., Peters, C., and Paus, R. (2002) *Am. J. Pathol.* **160,** 1807–1821
39. Benavides, F., Starost, M. F., Flores, M., Gimenez-Conti, I. B., Guenet, J. L., and Conti, C. J. (2002) *Am. J. Pathol.* **161,** 693–703
40. Candi, E., Tarcsa, E., Idler, W. W., Kartasova, T., Marekov, L. N., and Steinert, P. M. (1999) *J. Biol. Chem.* **274,** 7226–7237
41. Tarcsa, E., Marekov, L. N., Andreoli, J., Idler, W. W., Candi, E., Chung, S. I., and Steinert, P. M. (1997) *J. Biol. Chem.* **272,** 27893–27901
42. Hitomi, K., Ikeda, N., and Maki, M. (2003) *Biosci. Biotechnol. Biochem.* **67,** 2492–2494
43. Kim, H. C., Lewis, M. S., Gorman, J. J., Park, S. C., Girard, J. E., Folk, J. E., and Chung, S. I. (1990) *J. Biol. Chem.* **265,** 21971–21978
44. Barrett, A. J., Rawlings, N. D., and Woessner, J. F. (2004) *Handbook of Proteolytic Enzymes, Second Edition*, pp. 1097–1102, Elsevier Academic Press, London
45. Takahashi, M., Tezuka, T., and Katunuma, N. (1996) *Arch. Biochem. Biophys.* **329,** 123–126
46. Takahashi, M., Tezuka, T., Kakegawa, H., and Katunuma, N. (1994) *FEBS Lett.* **340,** 173–176
47. Hagemann, S., Gunther, T., Dennemarker, J., Lohmuller, T., Bromme, D., Schule, R., Peters, C., and Reinheckel, T. (2004) *Eur. J. Cell Biol.* **83,** 775–780
48. Reinheckel, T., Hagemann, S., Dollwet-Mack, S., Martinez, E., Lohmuller, T., Zlatkovic, G., Tobin, D. J., Maas-Szabowski, N., and Peters, C. (2005) *J. Cell Sci.* **118,** 3387–3395
49. Egberts, F., Heinrich, M., Jensen, J. M., Winoto-Morbach, S., Pfeiffer, S., Wickel, M., Schunck, M., Steude, J., Saftig, P., Proksch, E., and Schutze, S. (2004) *J. Cell Sci.* **117,** 2295–2307